AD-A010 702

BEHAVIOR OF PRESSURE STABILIZED BEAMS UNDER LOAD

Earl C. Steeves

Army Natick Laboratory
Natick, Massachusetts

May 1975

Unclassified

SECURITY CLASSIFICATION OF THIS PAGE (When Data Entered)

REPORT DOCUMENTATION PAGE		READ INSTRUCTIONS BEFORE COMPLETING FORM
1. REPORT NUMBER 75–82–AMEL	2. GOVT ACCESSION NO.	3. RECIPIENT'S CATALOG NUMBER
4. TITLE (and Subtitle) "Behavior of Pressure Stabilized Beams Under Load"		5. TYPE OF REPORT & PERIOD COVERED 6. PERFORMING ORG. REPORT NUMBER
7. AUTHOR(s) Earl C. Steeves		8. CONTRACT OR GRANT NUMBER(s)
9. PERFORMING ORGANIZATION NAME AND ADDRESS US Army Natick Development Center Aero-Mechanical Engineering Laboratory Natick, Massachusetts 01760		10. PROGRAM ELEMENT, PROJECT, TASK AREA & WORK UNIT NUMBERS 6.11.01.A 1T161101A 07 91
11. CONTROLLING OFFICE NAME AND ADDRESS Same As Above		12. REPORT DATE May 1975 13. NUMBER OF PAGES 38
14. MONITORING AGENCY NAME & ADDRESS(if different from Controlling Office)		15. SECURITY CLASS. (of this report) Unclassified 15a. DECLASSIFICATION/DOWNGRADING SCHEDULE

16. DISTRIBUTION STATEMENT (of this Report)

Distribution of this document is unlimited.

17. DISTRIBUTION STATEMENT (of the abstract entered in Block 20, if different from Report)

18. SUPPLEMENTARY NOTES

19. KEY WORDS (Continue on reverse side if necessary and identify by block number)

Beams	Experimentation	Air Supported Structures	Field Shelters
Pressure	Load Carrying	Tentage	Mobile Equipment
Stabilization	Load Control	Design	Analysis
Deformation	Capacity	Loads	
Flexibility	Load Stabilizer	Shelters	

20. ABSTRACT (Continue on reverse side if necessary and identify by block number)

The utilization of pressure stabilized structural elements in tentage support structures requires techniques for the design of such elements. A theory has been developed and reported previously for carrying out such a design of pressure stabilized beams. In this report an experimental investigation of the behavior of pressure stabilized beams under load is described and the experimental results are correlated with predictions from the theory. This correlation establishes the validity of the theory for predicting the deformation and load carrying capacity of pressure stabilized beams.

DD FORM 1 JAN 73 1473 EDITION OF 1 NOV 65 IS OBSOLETE

PRICES SUBJECT TO CHANGE

Unclassified

SECURITY CLASSIFICATION OF THIS PAGE (When Data Entered)

FOREWORD

This work was carried out in response to the results of the systems analysis conducted in connection with the preparation of the QMDO for Functional Field Shelters. This analysis identified the pressure stabilized beam structural concept as being the most promising with regard to meeting the Army requirement for lightweight highly mobile tentage. This report presents results from a project initiated in FY71 to investigate the feasibility of this structural concept and to develop design data for pressure stabilized structural elements which will be used in the concept. Support for this project has been provided through the In-House Laboratory Independent Research program.

TABLE OF CONTENTS

LIST OF TABLES

LIST OF FIGURES

INTRODUCTION

A systems analysis of Army needs for shelters in the 1985 time frame revealed that the requirements for lightweight tentage of low package bulk with minimum setup and disassembly times might be most effectively achieved by a tent with a frame of highly pressurized (compared with present air supported tents) structural elements supporting a lightweight fabric barrier, as illustrated in Figure 1. Since the structural elements are pressure stabilized, they can be fabricated from lightweight, flexibile materials such as cloth, thus reducing the weight and bulk of the transport configuration. The use of bladders or coated fabric for these elements should provide sufficient air retention capability to eliminate the need for the continuous air supply required by current air supported tents.

The use of higher pressure would allow the reduction of the number and cross section size of the supporting elements in comparison with present double wall air supported tents. However, the degree to which this could be accomplished was not known because insufficient data were available on the manner in which the strength and deformation of pressure stabilized structural elements depends on pressure level, element geometry and mechanical properties of the skin material. As a result an investigation to develope the data necessary for the design of tents using pressure stabilized structural elements was undertaken. The approach followed in this investigation was the development of a theory to predict the deformation behavior under load and the verification of this theory through correlation with experimental results. A detailed presentation of the theory is given in reference (1) along with a general discussion of the theoretical results. The purpose of this report is the presentation of the experimental procedures and results for the behavior of pressure stabilized beams under load and their correlation with the theoretical predictions to demonstrate the validity of the theory.

Previous experimental work of a similar nature (reference 2) concerned the behavior of inflated coated metal fabric beams subjected to pure bending, shear loading and torsion. This work covered the pressure range from 0 to 82,737 Pa (0 to 12 psi) and beams with length to diameter ratio ranging from 14 to 16. This left considerable need for extending the range of geometry and inflation pressure levels so that the accuracy of theoretical prediction could be established by comparison with experimental results. In addition, it was desired to use materials typical of those envisioned for use in tentage structures.

Experimental procedures to measure the strength and deformation of beams under load and to determine the mechanical behavior of the skin materials are described. The material stiffness in tension and shear are shown as a function of stress level. The experimental results presented for beams depict the flexibility and wrinkling load as a function of pressure level for beams subjected to a concentrated load at mid span. Comparison of these experimental results with theoretical predictions are also shown.

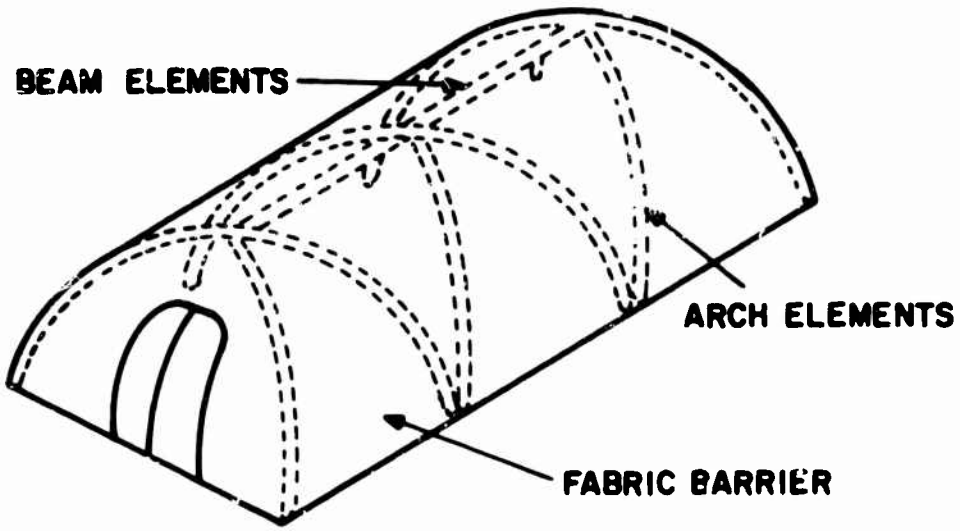

Figure 1. Tent Concept Using Pressure Stabilized Structural Elements

EXPERIMENTAL PROCEDURES

The experimental investigation was carried out in two phases; the first being loading tests of pressure stabilized beams to confirm the validity of the bending theory developed in reference 1 and the second being the measurement of the elastic modulus and shear modulus of the fabric materials used in the fabrication of the beams.

Beam Bending Tests

The objective of these tests was to measure the deformation behavior and load carrying capacity of pressure stabilized beams for several geometries, inflation pressure levels and materials. The flexibility, that is the deflection per unit load, was taken as the measure of the deformation and the wrinkling load was used as the measure of load carrying capability. The wrinkling load is defined as the load at which the maximum compressive stress due to bending is equal in magnitude to the tensile stress due to pressurization; thus any further increase in the bending load would cause wrinkling of the fabric.

A schematic illustration of the experimental setup for measuring the deformation behavior and load carrying capacity of beams in bending is shown in Figure 2 and a photograph of the actual test apparatus is shown in Figure 3. The beams were fabricated from woven fabric with a butyl rubber inner tube used for a bladder. The fabric cylinders were fabricated from flat stock by sewing a seam along the length of the cylinder as is evident in Figure 3. Experimental results were obtained for beams made of vinyl-coated nylon and heat set dacron fabrics. The characteristics of these fabrics are given in MIL-C-43086B Type I and MIL-C-43347D Type I respectively. The beam ends were sealed for pressurization by clamping the fabric and bladder in a grooved end cap with a hose clamp. Details of this sealing technique are shown in Figure 4. Beams of 0.6, 0.9 and 1.2 m length all having a 0.064 m diameter cross section were tested for both the nylon and dacron fabrics. The experiments cover the pressure range from 34,500 to 207,000 Pa (5-30 psi).

As shown in Figure 3 the test apparatus was mounted in a Tinius-Olsen testing machine which was used as a loading device. Concentrated loads were applied at the center of the beam using a webbing 2.54 cm wide wrapped around the periphery of the beam. This webbing was attached to the moving head of the testing machine with a 0.0063 m diameter steel cable. Uniform rate loading was used with the load magnitude being measured by a strain gauge load transducer the output of which was recorded on a strip chart recorder after amplification. The loading rate, although not specifically measured, was felt to be sufficiently slow so as to preclude significant influence of any rate effects exhibited by the nylon and dacron skin materials. Typical loading times from no load to wrinkling load were 10-20 sec. The displacement was measured at the point of load application using a direct current linear variable differential transformer with its output

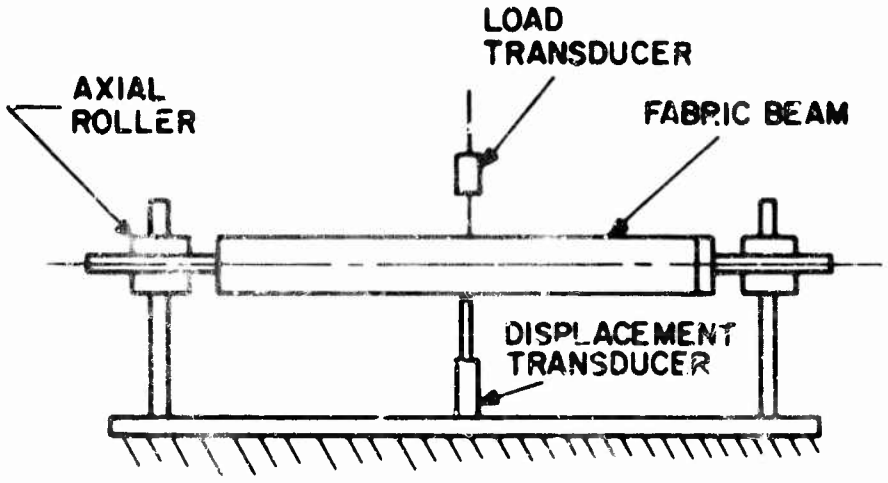

Figure 2. Schematic Diagram of Experimental Apparatus

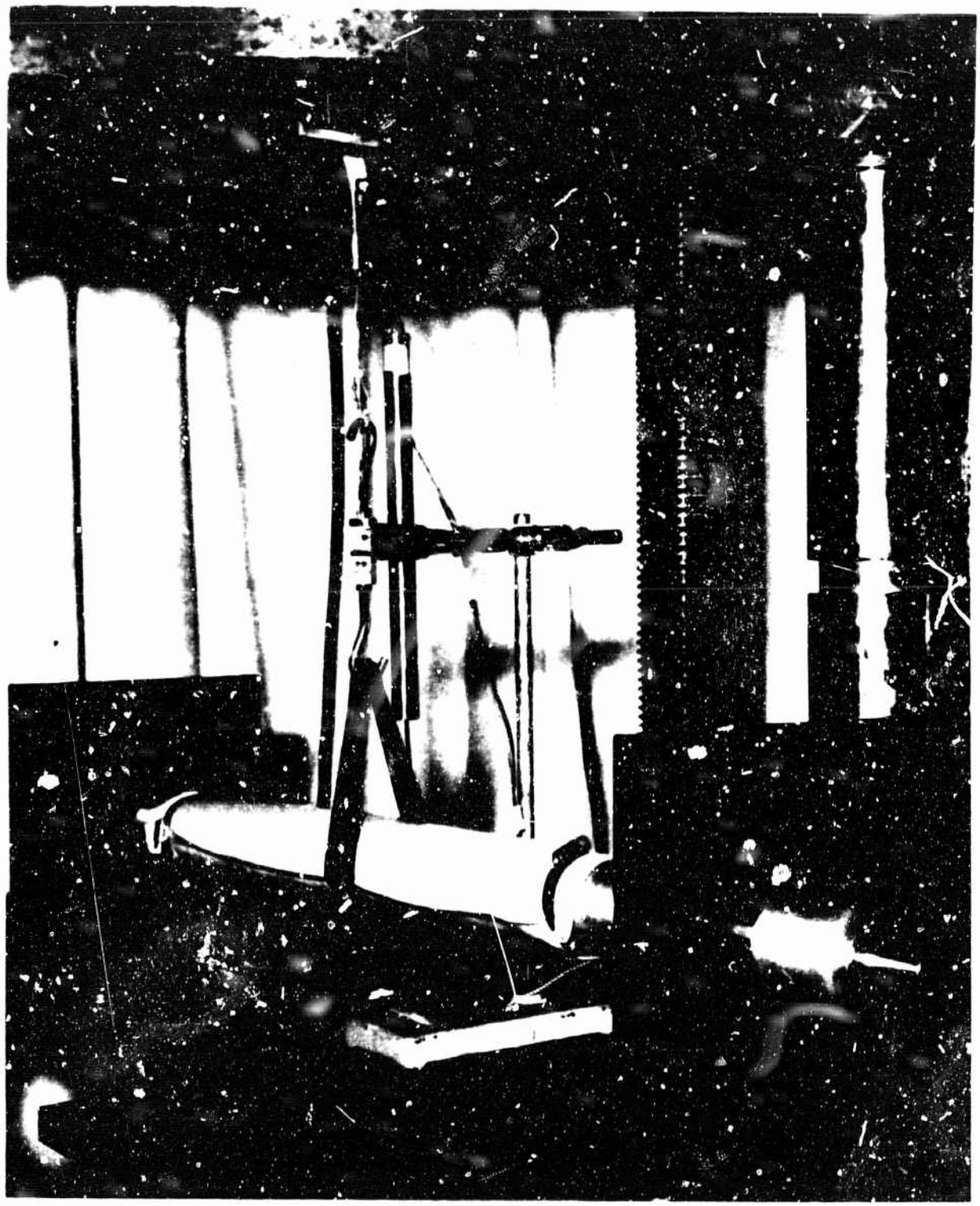

Figure 3. Beam Bending Test Apparatus

Figure 4. Detail of Beam-Endcap Asser

also recorded on a strip chart recorder. Typical outputs for both load and displacement are presented in Figure 5. As shown 3 tests were conducted at each pressure level. The ends of the beam were supported normal to the beam axis to prevent transverse deflection of the beam ends and the ends were restrained against rotations about an axis normal to the beam axis to simulate fixed-end or clamped conditions. The beam end supports were mounted in axial rollers so that the ends were free to move parallel to the beam axis.

To facilitate the comparison of the experimental results obtained, the measured force and displacement were converted to the nondimensional parameters used in the theory. The measured transverse displacement $\bar{W}$ is converted to nondimensional form by the relation:

$$W = \bar{W}/a$$

where W is the nondimensional displacement and a is the cross section radius. Conversion of the measured force F to the nondimensional force parameter g is illustrated in Figure 6. The nondimensional force parameter g is defined as

$$g = \frac{1}{\bar{C}_{11}\pi} \int_0^{2\pi} G(\Theta)\mathrm{Sin}(\Theta)\, d\Theta$$

where $\bar{C}_{11}$ is a reference value of the elastic modulus and $G(\Theta)$ is a line load distribution on the periphery of the beam as illustrated in Figure 6. Since the webbing contacts the beam over only a portion of its circumference the limits on the integral can be changed giving

$$g = \frac{1}{\bar{C}_{11}\pi} \int_{-3\pi/2+\alpha}^{\pi/2-\alpha} G(\Theta)\mathrm{Sin}(\Theta)\, d\Theta$$

The line load also acts on the webbing which must be in equilibrium and therefore the following relation must hold:

$$F = \int_{-3\pi/2+\alpha}^{\pi/2-\alpha} G(\Theta)\mathrm{Sin}(\Theta)\, a\, d\Theta$$

Comparison of the expressions for g and F reveals the following relation :

$$g = F/\bar{C}_{11}\pi a$$

which is the desired expression for nondimensionalizing the force parameter.

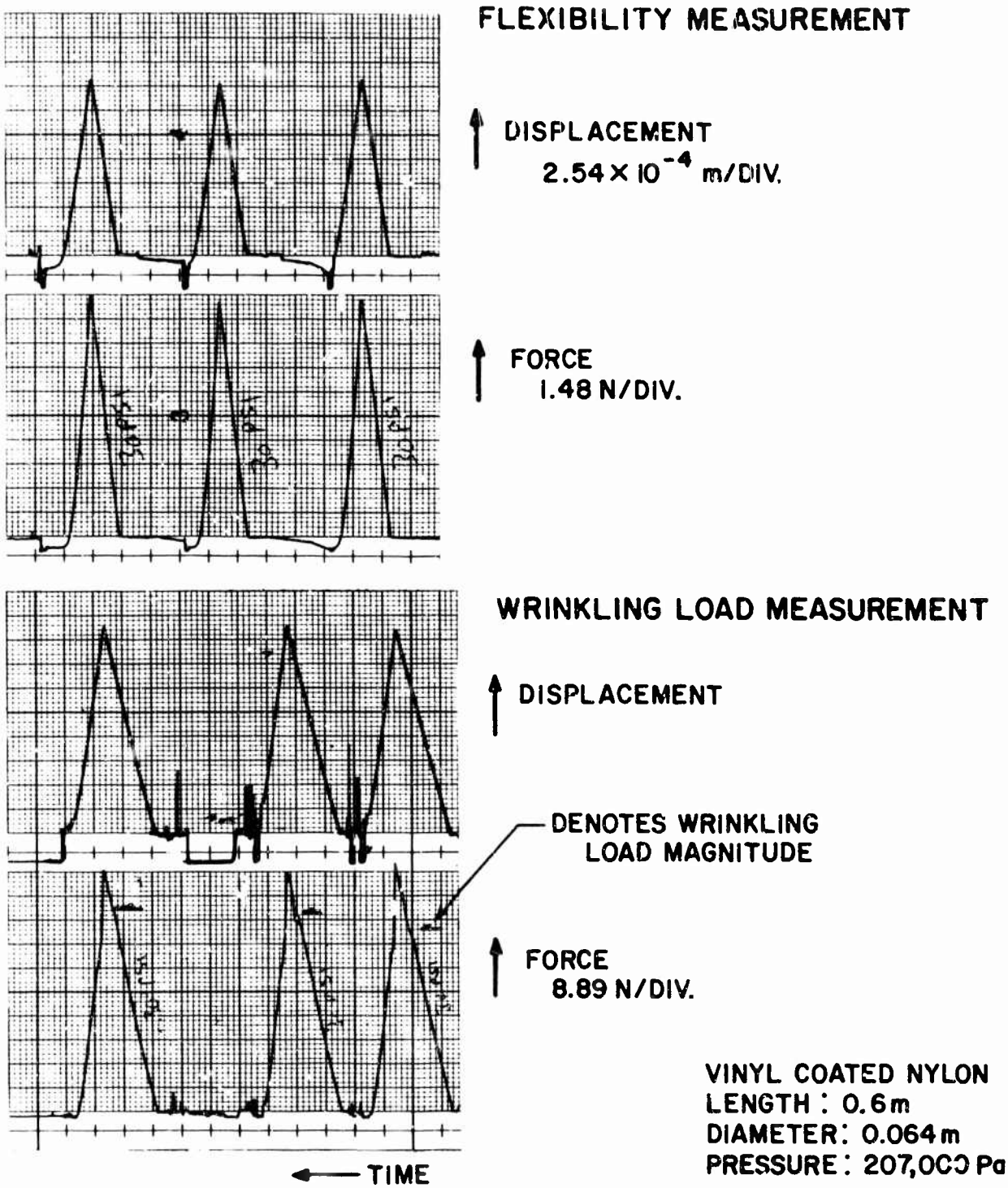

Figure 5. Typical Recordings of the Force and Displacement From Bending Tests

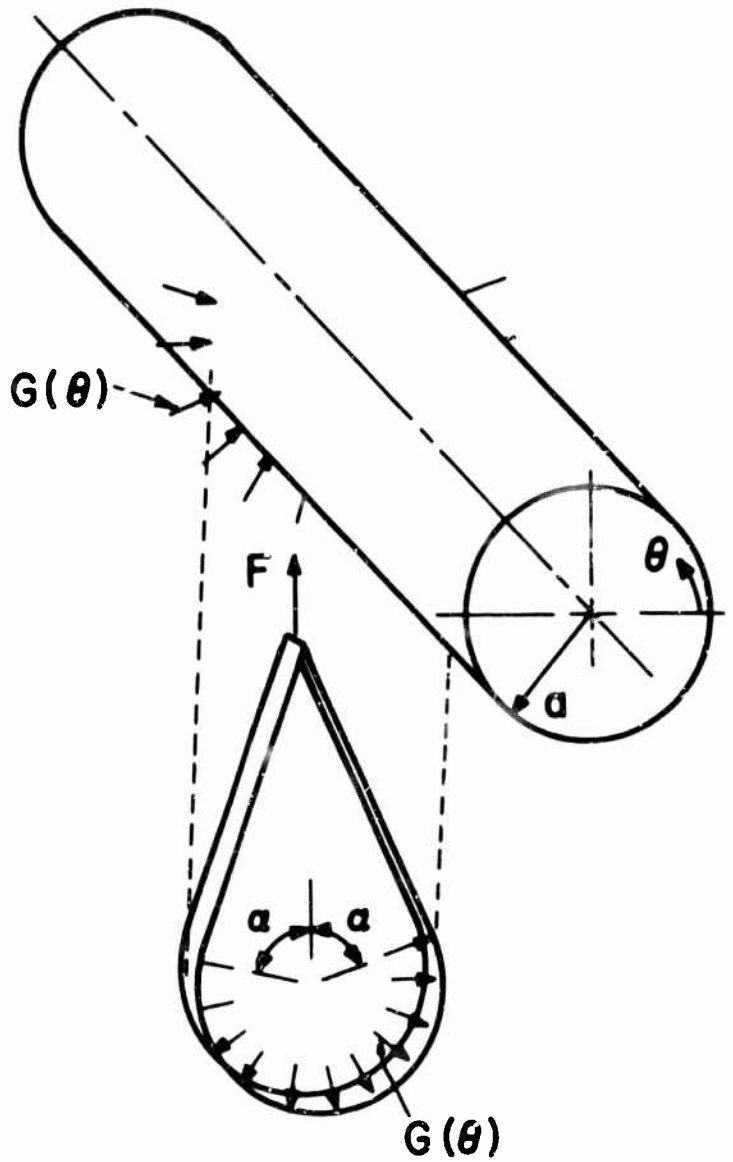

Figure 6. Beam Loading Technique

Using these expressions for conversion of the physical measurements to nondimensional form we can obtain expressions for the nondimensional wrinkling load and flexibility. If the subscript w denotes wrinkling then the nondimensional wrinkling load is given in terms of the physical wrinkling load as:

$$g_W = F_W/\pi a\bar{C}_{11}$$

The magnitude of F_W is determined experimentally by finding the value of F for which the loading curve becomes nonlinear. As is evident from Figure 5 this nonlinearity takes the form of a discontinuity or jump during which the load remains essentially constant and the deformation continues at a uniform rate. The discontinuity occurs in the loading curve because the testing machine imposes a uniform rate of deformation.

The flexibility is the transverse displacement due to a unit load which in nondimensional form is:

$$\gamma = W/g$$

Substituting the expressions for W and g gives the following expression for the nondimensional flexibility in terms of the measured force and displacement:

$$\gamma = \pi\bar{C}_{11}\,\bar{W}/F$$

Determination of Material Properties

To make a theoretical prediction of the experimental results obtained using the procedures described above it was necessary to know the elastic and shear moduli of the beam materials. These moduli or stiffnesses were determined from the results of a tension test and torsion test respectively. Although these tests were very similar to those commonly used they were performed on specimen in their pressurized state of stress. Testing in this manner yields stiffnesses relative to a state of stress very close to that present in the bending tests. That is, uniaxial tension or shear superimposed on biaxial tension resulting from internal pressure in the cylinderical specimen. The moduli were measured using relatively small excursion from the pressurized state of stress and the behavior was assumed to be linear over these excursions. Thus for a given value of pressure the elastic and shear moduli are constants. However, because of the significance of biaxial stress effects in fabrics and the nonlinear stress-strain behavior of nylon and dacron these moduli were in general found to be a function of the pressure level. This testing procedure had the additional advantage of yielding the moduli of the fabric skin-butyl rubber bladder composite, and although the bladder is thought to make little contribution to the stiffness any contribution is included.

Elastic Modulus. As indicated above the elastic modulus was determined from the results of a tension test which is shown schematically in Figure 7. The test is performed in the usual manner, applying an axial force F and measuring its magnitude along with the corresponding elongation, e. The theory (reference 1) requires knowledge of the constant, C_{11}, relating the stress resultant, N_{11}, and the strain, ϵ_{11} as

$$N_{11} = C_{11}\epsilon_{11}$$

Thus C_{11} is the slope of the stress resultant – strain curve and can be computed from the force-elongation curve generated from the tension test by the expression

$$C_{11} = l_g \, \Delta F/2\pi a \, \Delta e$$

where ΔF and Δe are respectively increments of applied force and specimen elongation and l_g is the specimen gauge length and a is the specimen radius. In the tests conducted gauge length and specimen radius respectively were 0.165-m and 0.032-m. Typical force and elongation plots from these tests are shown in Figure 8.

Shear Modulus. The shear modulus was determined from the results of a torsion test as shown schematically in Figure 9. This test is performed by applying a torque, T, about the axis of the cylinder and measuring the rotation, ϕ, of the end of the cylinder corresponding to that torque. The theory (reference 1) requires the constant C_{33} relating the shear stress resultant, N_{12}, to the shear strain, ϵ_{12}, as

$$N_{12} = C_{33}\epsilon_{12}$$

Again C_{33} is the slope of the stress resultant-strain curve and can be computed from the torque-rotation curve generated from the torsion test by the expression

$$C_{33} = l_g \, \Delta T/2\pi a^3 \, \Delta \phi$$

where ΔT and $\Delta\phi$ are respectively increments of applied torque and specimen rotation. The parameters l_g and a are as defined above and for the test conducted have the values 0.25-m and 0.032-m respectively. Typical torque and rotation plots from these tests are shown in Figure 10.

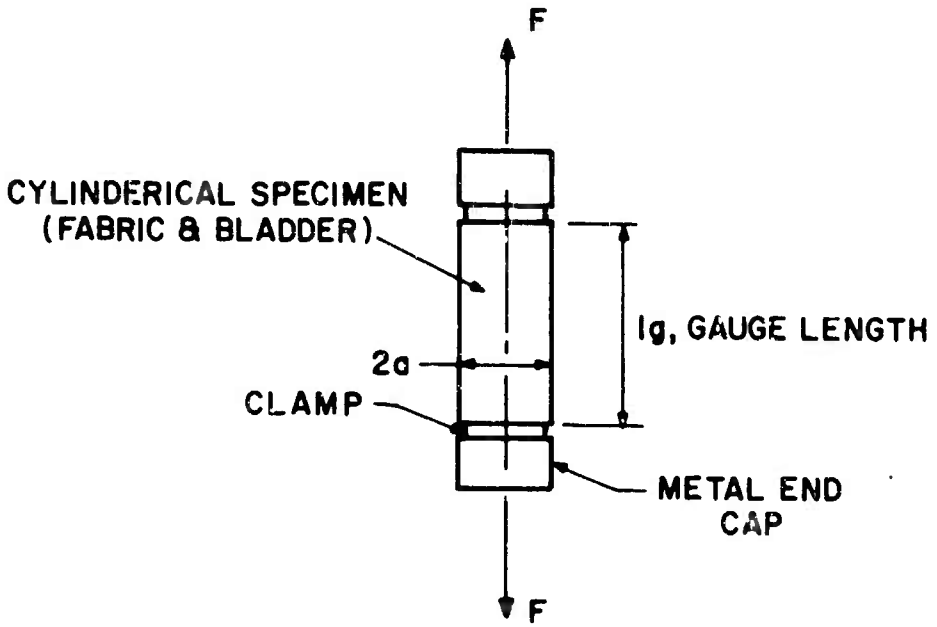

Figure 7. Schematic Diagram of the Tension Test

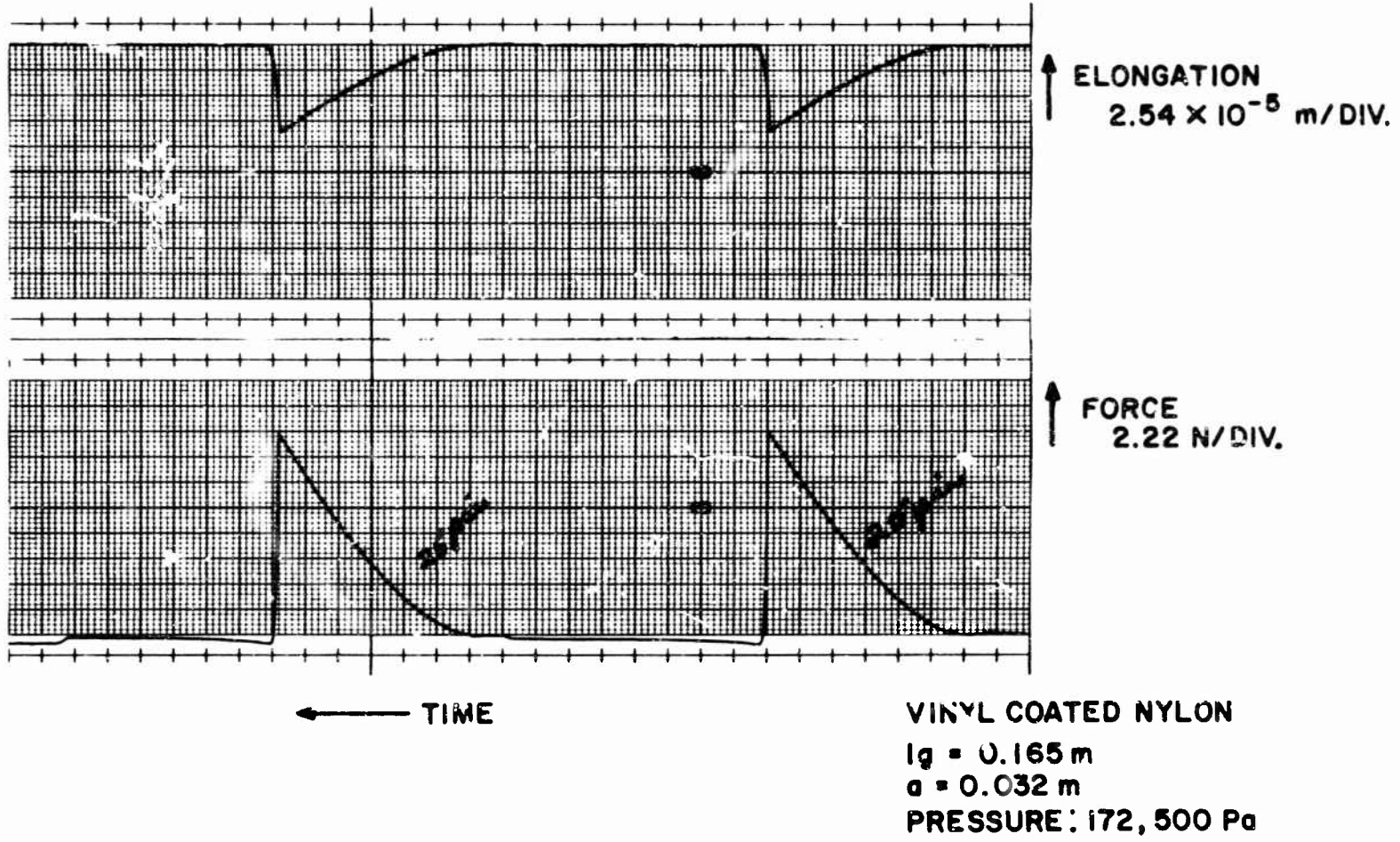

Figure 8. Typical Force and Elongation Recordings From Tension Test

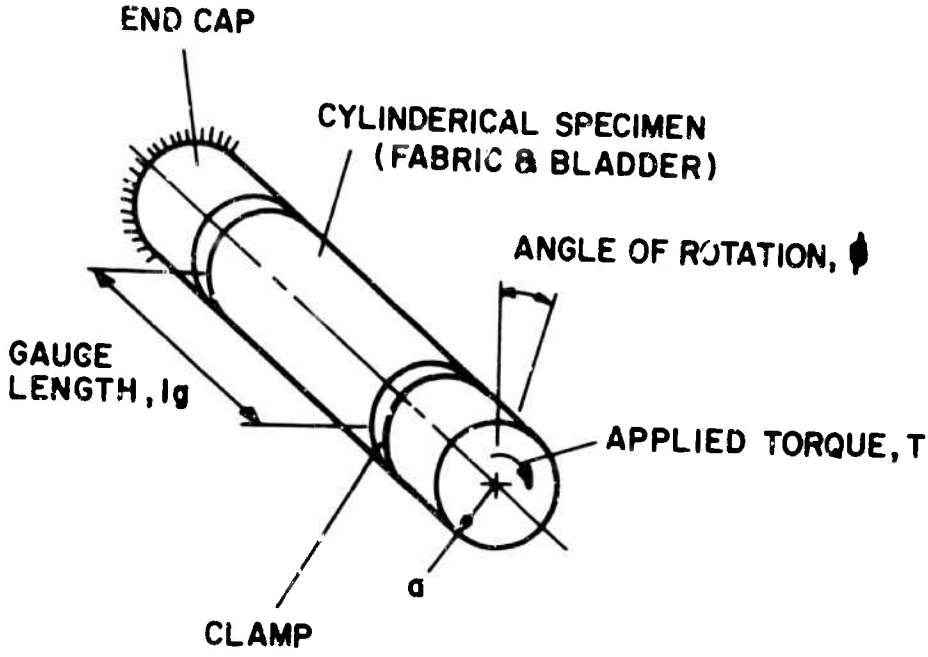

Figure 9. Schematic Diagram of the Torsion Test

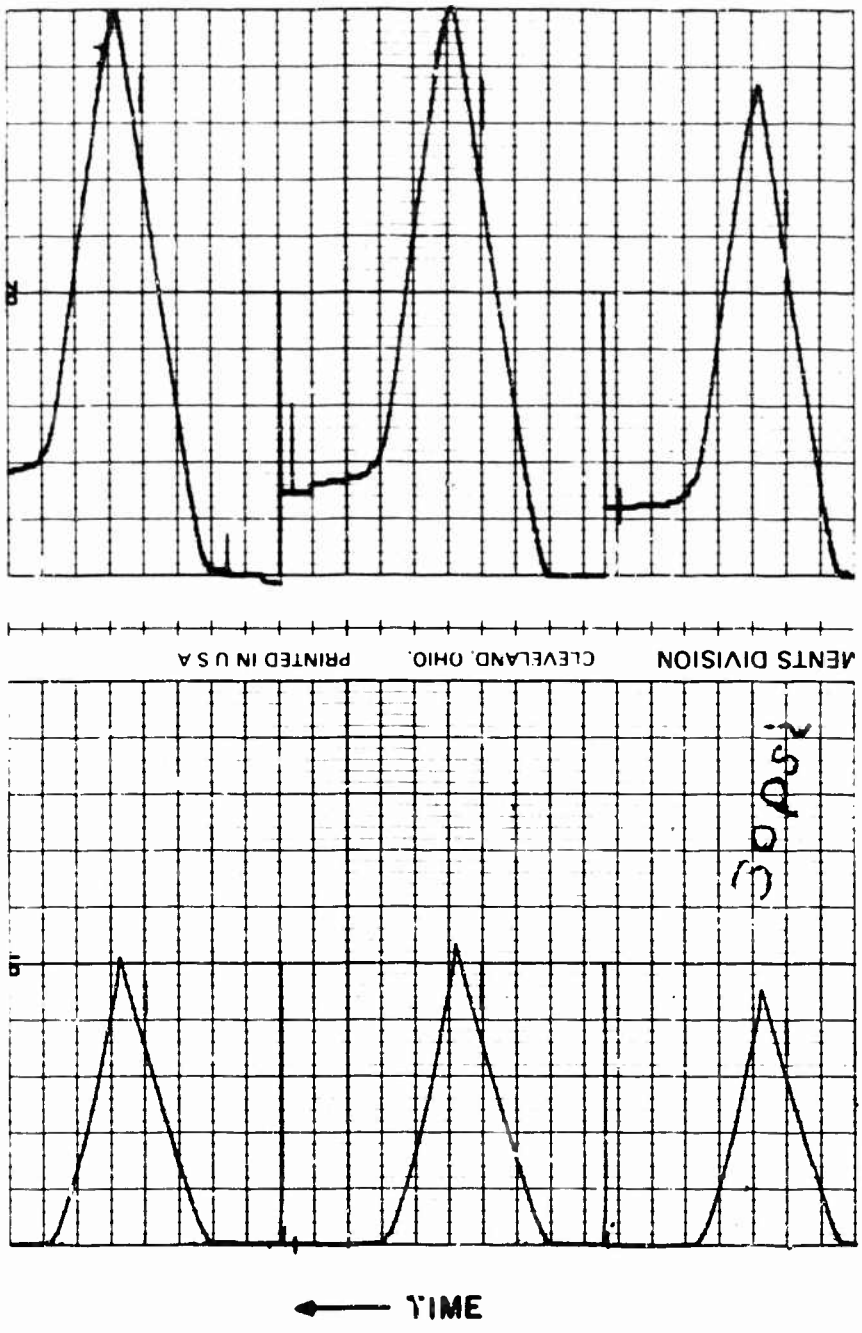

Figure 10. Typical Torque and Rotation Recordings From Torsion Test

DISCUSSION OF RESULTS

In this section we will present the experimental results obtained with the procedures just described and compare the experimental results on beam performance to the predictions of the theory previously developed and reported in reference 1.

Material Properties

The behavior of the elastic modulus and the shear modulus as a function of pressure level are shown in Figure 11 where the symbols denote the average of the values given for each pressure in Tables I and II. These results are presented in the nondimensional form used in the theory. The moduli and pressure parameter are nondimensionalized using $\bar{C}_{11}$ which represents the magnitude of C_{11}, the elastic modulus, for zero pressure. The pressure parameter which is used throughout this section is the nondimensional axial stress resultant in the cylinder due to internal pressure loading and is given in terms of the pressure, P, and the cross section radius, a, as:

$$n = Pa/2\bar{C}_{11}$$

where n denotes the pressure parameter. In Figure 11 the experimental results for both the nylon and dacron fabrics are denoted by the symbols and the least squares linear fit of this data used in the theory are shown both graphically and mathematically. Also given are the values of $\bar{C}_{11}$ as determined from the linear fit. Examination of this data indicates that the elastic modulus of nylon is independent of pressure while that for dacron and the shear modulus for both materials vary with pressure. It is also apparent that the shear modulus or stiffness of the fabrics is small being from 2 to 12 percent of the elastic modulus.

Behavior of Beams Under Load

The results of the bendings tests for beams having length to diameter ratios of approximately 9, 14 and 18 are shown graphically in Figures 12, 13 and 14. The experimental data on which these plots are based is presented in Tables III to VIII. Each of these figures contain plots of the nondimensional flexibility and the nondimensional wrinkling load as functions of the nondimensional pressure parameter. The experimental results are denoted by the symbols and the curves represent the behavior predicted by the theory presented in reference 1. The flexibility is the deformation per unit load and the wrinkling load is defined as the load for which the maximum compressive stress resulting from bending is equal in magnitude to the tensile stress resulting from pressurization; thus any further increase in the bending load would cause wrinkling of the fabric. The flexibility and the wrinkling load are then respectively measures of the deformation behavior and the load carrying capaciaty.

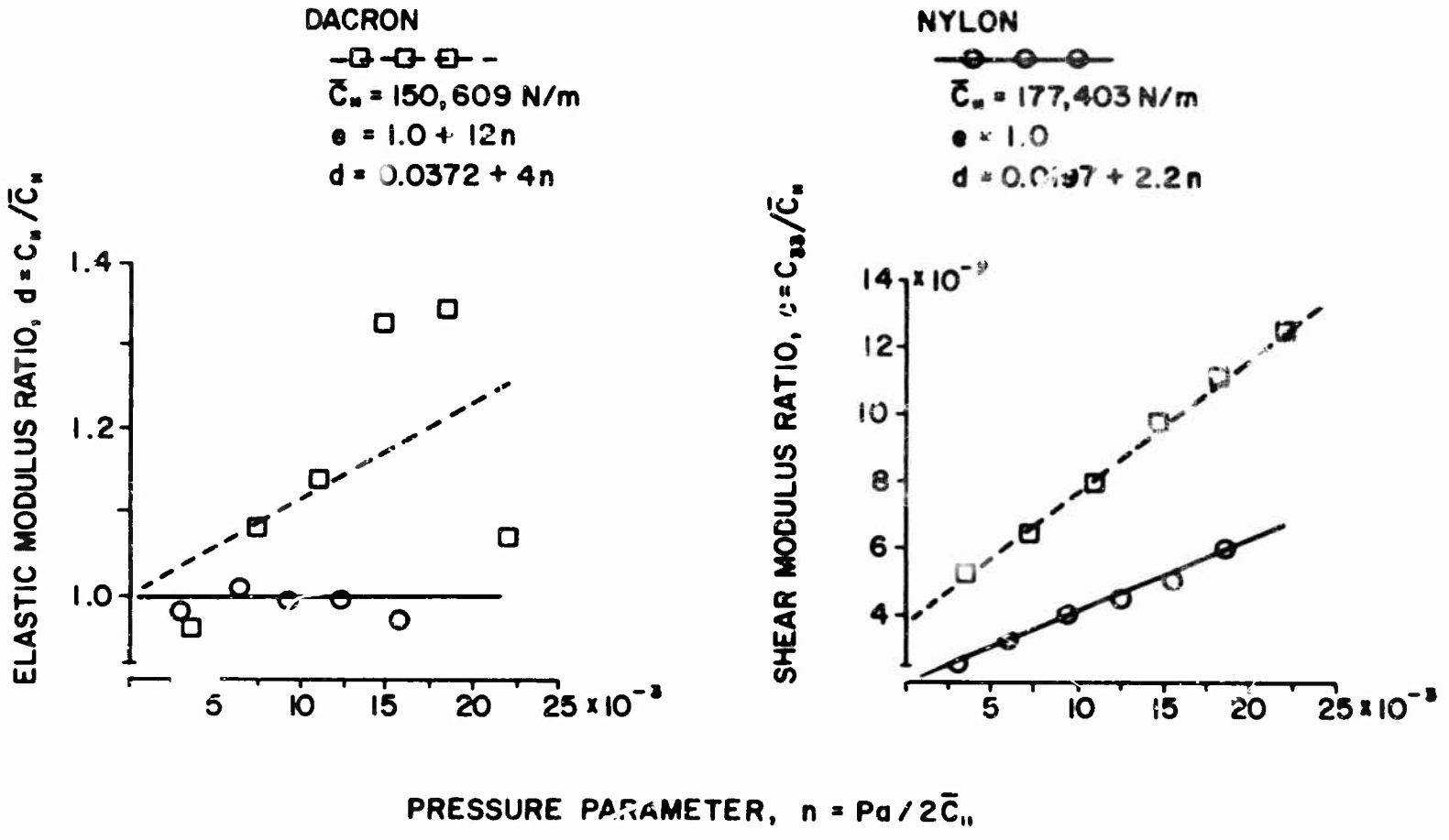

Figure 11. Elastic Modulus and Shear Modulus Ratios as a Function of Pressure

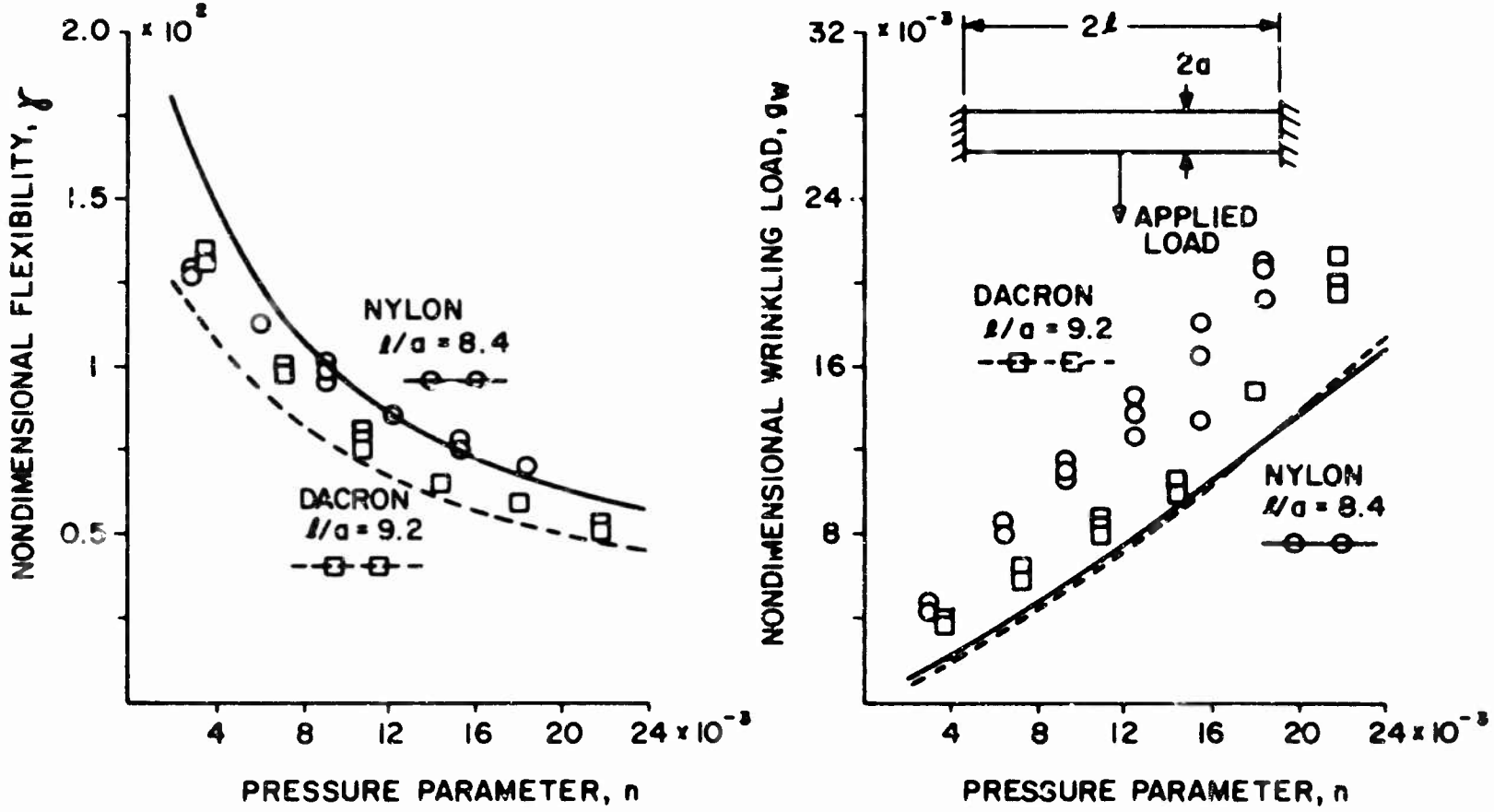

Figure 12. Beam Flexibility and Wrinkling Load as a Function of Pressure ($\ell/a \cong 9$)

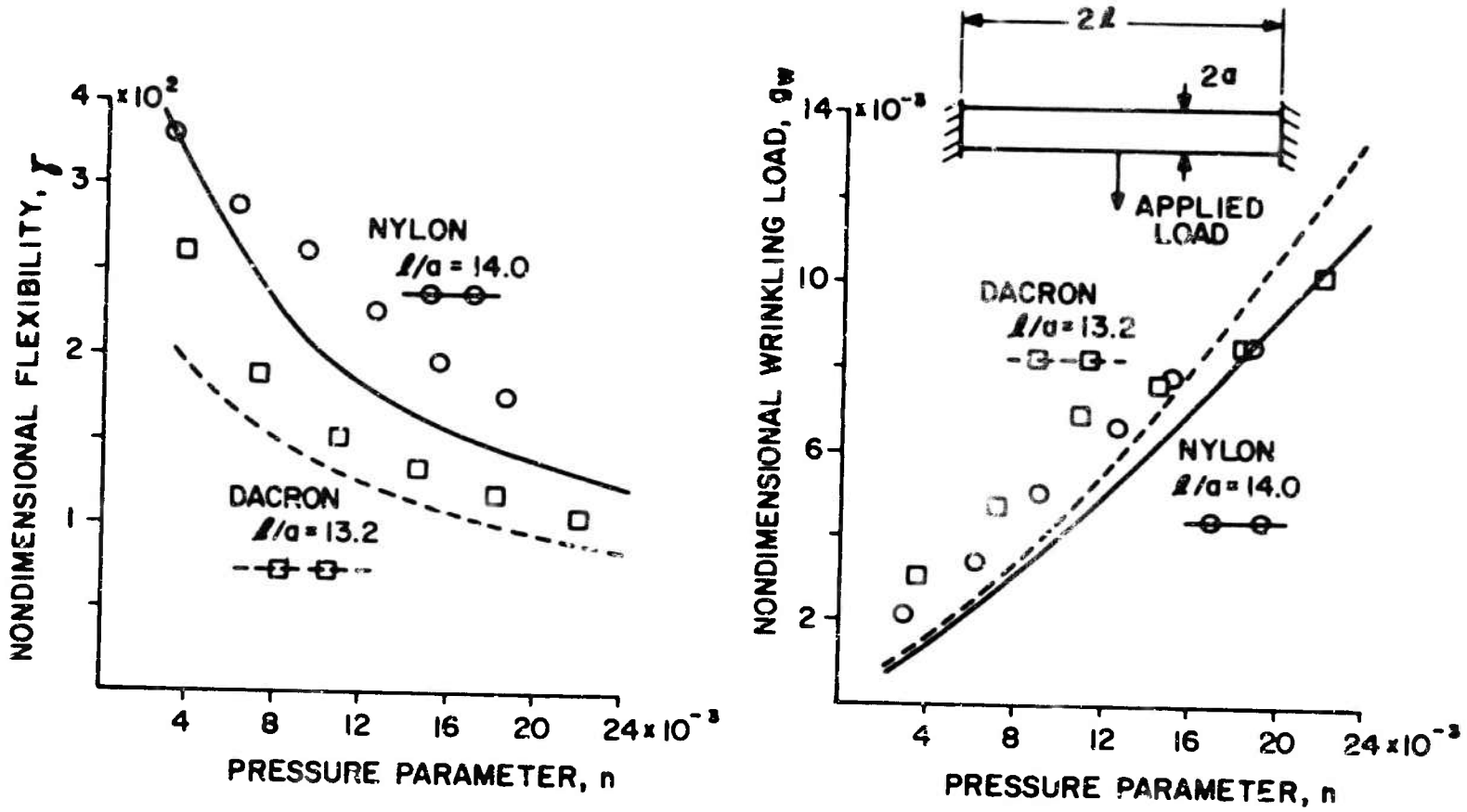

Figure 13. Beam Flexibility and Wrinkling Load as a Function of Pressure ($\ell/a \cong 14$)

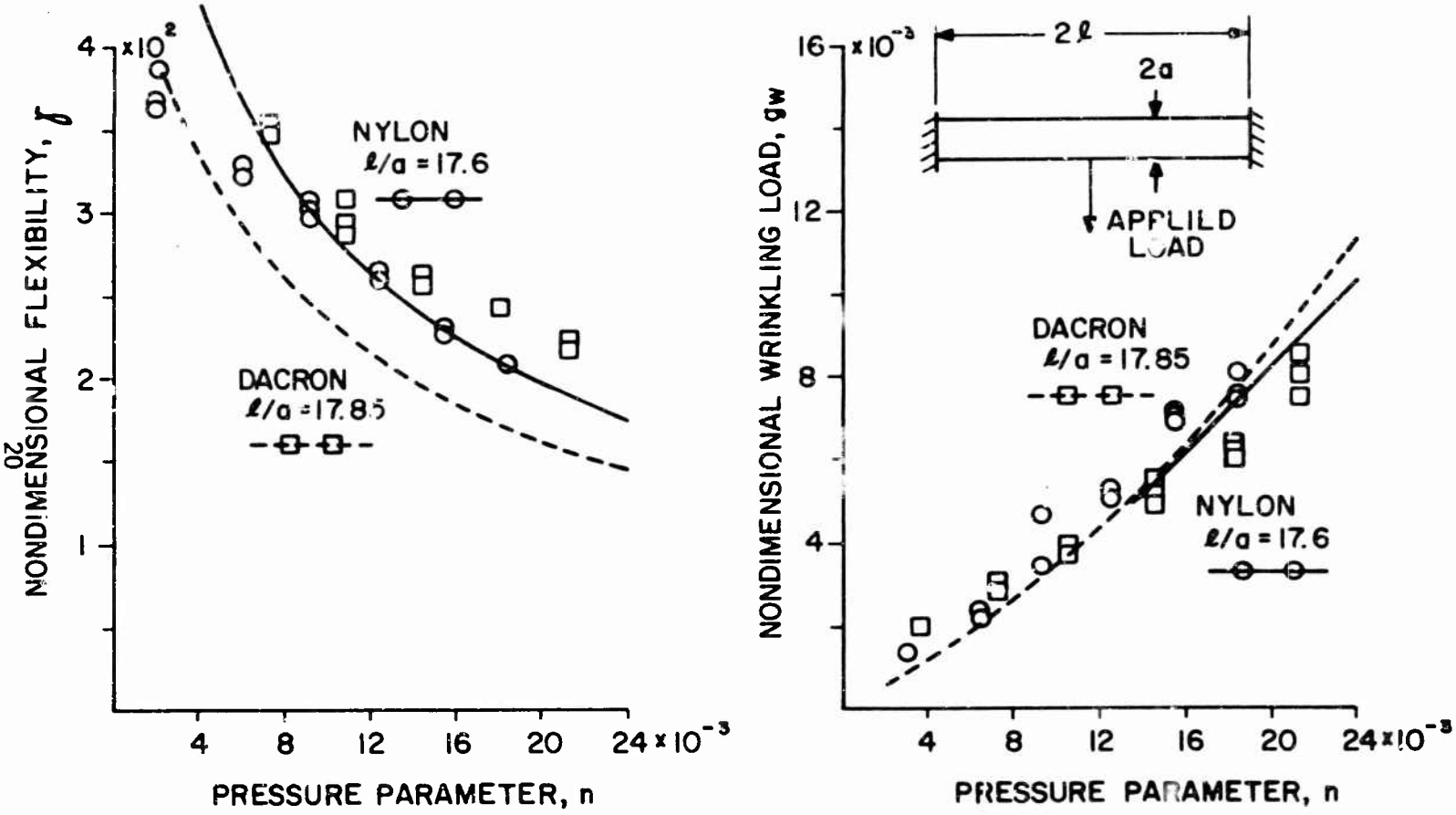

Figure 14. Beam Flexibility and Wrinkling Load as a Function of Pressure ($\ell/a \cong 18$)

For all three geometries both the theoretical and experimental results show the flexibility varying inversely with the pressure and the wrinkling load increasing monotonically with pressure. It can be seen clearly that the wrinkling load increases more rapidly than a linear function with pressure and it was shown in reference 1 that for the uniformly loaded beam the wrinkling load increased quadratically with the pressure.

The agreement between the experimental results and the theoretical predictions is acceptable. However, two exceptions are observed, these being the rather poor agreement between experimental data and prediction in the wrinkling load for the shortest nylon beam and in the flexibility for the longest dacron beam. However, in both cases the companion comparisons, that is the flexibility for the shortest nylon beam and the wrinkling load for the longest dacron beam, are in good agreement. Thus these cases of poor agreement are felt to be some anomalous behavior in the experimental results and not poor predictions from the theory. The differences between theory and experiment can be attributed to a number of factors, namely, the likely difference between the degree of fixity of end supports assumed in the theory and that attainable experimentally, possible nonlinear behavior of the material under stress and effect of changes in the orientation of the fabric caused by twisting of the cylinder when pressurized. This last effect is unique to fabric-type structures and is thought to be the result of skewness or nonorthogonality of the yarns. The problem of obtaining truely fixed ends experimentally is a common one in structural testing. Experimental simulations are typically more flexible due to the difficulty of restrainting rotation. Thus, it is expected that the experimental results will have higher flexibilities than the theory and this is generally true for the results presented.

The differences between the results for the nylon and dacron beams shown on each of Figures 12, 13 and 14 are the result of the small geometric differences and the difference in the elastic and shear moduli as shown on Figure 11.

To see how well the theory represented the distribution of displacement along the length of the beam experimental measurements of displacement were made at 5 points on the longest nylon beam. The results and the comparison with theory are shown in the table. Because the objective was to compare distributions the experimental and theoretical results have been normalized independently by dividing by the midspan (x/l = 0.0) deflection. These results indicate that the theory represents the distribution quite well. The largest difference between theory and experiment occurs near the fixed end and is believed caused by the incomplete fixity of the ends against rotation.

	W/W_o	
x/l	Exp.	Theory
1.0	–	0.0
0.8	0.23	0.17
0.6	0.46	0.39
0.4	0.64	0.61
0.2	0.83	0.83
0.0	1.0	1.0

The good agreement between theory and experiment for beams of two different materials and over a range of geometries and pressure levels establishes the validity of the theory described in reference 1 for predicting the deformation and load carrying capacity of pressure stabilized beams.

CONCLUSIONS

Experimental and theoretical results have been presented depicting the behavior of pressure stabilized beams under load. The agreement between these experimental and theoretical results establishes that the theory reported in reference 1 which is based on linearization about the pressurized state, elementary beam-type displacement approximations and utilizing a linear continuum mechanics stress-strain law for fabric materials is adequate for the prediction of the deformation and load carrying capacity of pressure stabilized beams.

TABLE I

ELASTIC AND SHEAR STIFFNESS DATA FOR DACRON FABRIC

Pressure		Elastic Stiffness			Shear Stiffness		
P, Pa	n, Nondim.	Force ΔF, N	Elongation Δe,m	Elastic modulus C_{11}, N/m	Torque ΔT, N-m	Rotation $\Delta\phi$, rad.	Shear modulus C_{33}, N/m
34.5×10^3	3.66×10^{-3}	135.8	0.91×10^{-3}	141.4×10^3	4.54	0.746	7883.3
		135.8	0.89	144.6	4.61	0.754	7918.9
		141.6	0.94	142.7	4.61	0.754	7919.9
69.0	7.32	141.6	0.84	159.7	5.55	0.761	9447.2
		139.6	0.81	163.3	5.58	0.754	9586.4
		140.6	0.81	164.5	5.52	0.739	9675.8
103.5	10.98	139.6	0.76	174.0	6.05	0.709	11053.6
		140.6	0.79	168.6	5.93	0.627	12251.2
		135.8	0.79	162.9	5.96	0.627	12251.2
138.0	14.64	134.9	0.61	209.5	6.21	0.559	14390.4
		135.8	0.66	194.9	5.98	0.522	14839.7
		125.3	0.61	194.6	5.96	0.522	14790.0
172.5	18.3	148.3	0.66	212.9	6.18	0.478	16747.6
		126.3	0.61	196.2	6.03	0.463	16870.6
		139.6	0.68	194.5	6.03	0.463	16870.6
207.0	21.96	139.6	0.81	163.3	5.87	0.403	18868.0
		137.8	0.81	161.2	5.93	0.418	18376.9
		137.8	0.81	161.2	6.05	0.425	18439.9

TABLE II

ELASTIC AND SHEAR STIFFNESS DATA FOR NYLON FABRIC

Pressure		Elastic Stiffness			Shear Stiffness		
P, Pa	n, Nondim.	Force ΔF, N	Elongation Δe, m	Elastic modulus C_{11}, N/m	Torque ΔT, N-m	Rotation $\Delta\phi$, rad.	Shear modulus C_{33}, N/m
34.5×10^3	3.11×10^{-3}	95.6	0.49×10^{-3}	160.2×10^3	1.76	0.493	4404.2
		93.4	0.41	187.1	1.21	0.334	4469.3
					2.57	0.644	4923.2
69.0	6.22	88.9	0.42	173.8	2.97	0.620	5909.8
		88.9	0.41	178.0	2.02	0.437	5702.6
					3.37	0.731	5687.4
103.5	9.33	102.3	0.49	171.4	3.51	0.636	6808.5
		88.9	0.41	178.0	3.11	0.525	7308.1
					2.64	0.461	7064.9
138.0	12.44	88.9	0.43	169.7	4.46	0.692	7951.2
		88.9	0.41	178.0	2.70	0.413	8065.2
					3.78	0.588	7930.8
172.5	15.55	88.9	0.43	169.7	4.19	0.556	9297.0
		88.9	0.43	169.7	4.73	0.652	8949.9
					3.51	0.477	9078.0
207.0	18.66				3.92	0.437	11066.4
					4.73	0.540	10806.2
					4.73	0.556	10495.2

TABLE III

BENDING TEST DATA FOR DACRON BEAM WITH $\rho = 9.2$

Pressure		Flexibility			Wrinkling Load	
P, Pa	n, Nondim.	Force F, N	Displacement $\bar{W}$, m	Nondim. Flexibility γ	F_{wr}, N	q_{wr}, Nondim.
34.5×10^3	3.66×10^{-3}	37.81	1.05×10^{-2}	131.4	57.8	3.81×10^{-3}
		35.58	0.99	131.6	60.1	3.97
		36.92	1.05	134.6	62.3	4.11
69.90	7.32	51.15	1.08	99.9	97.9	6.47
		50.26	1.05	93.8	91.2	6.02
		51.15	1.05	97.1	93.4	6.17
103.5	10.98	70.73	1.19	79.6	133.4	8.81
		72.06	1.16	76.2	120.1	7.93
		71.17	1.18	78.4	129.0	8.52
138.0	14.64	74.28	1.03	65.6	160.1	10.57
		73.84	1.03	66.0	160.1	10.57
		74.23	1.02	64.9	146.8	9.69
172.5	18.3	72.50	0.89	58.1	222.4	14.69
		72.06	0.88	57.8	222.4	14.69
		69.84	0.88	59.6	222.4	14.69
207.0	21.96	72.06	0.79	51.9	293.6	19.39
		69.84	0.79	53.5	320.3	21.15
		72.51	0.79	51.6	302.5	19.98

TABLE IV

BENDING TEST DATA FOR DACRON BEAM WITH $\rho = 13.2$

Pressure		Flexibility			Wrinkling Load	
P, Pa	n, Nondim.	Force F, N	Displacement $\bar{W}$, m	Nondim. Flexibility γ	F_w, N	q_w, Nondim.
34.5×10^3	3.66×10^{-3}	20.02	1.15×10^{-2}	271.8	40.0	2.64×10^{-3}
		21.48	1.17	257.7	44.5	2.94
		21.48	1.14	251.1	44.5	2.94
69.0	7.32	29.67	1.14	181.8	68.9	4.55
		28.94	1.17	184.9	71.2	4.70
		28.91	1.14	186.6	66.7	4.41
103.5	10.98	37.36	1.15	145.6	93.4	6.17
		37.05	1.17	149.4	108.9	7.19
		34.83	1.15	156.2	102.3	6.76
138.0	14.64	41.50	1.17	133.4	111.2	7.34
		39.54	1.10	131.6	108.9	7.19
		41.77	1.17	132.5	120.1	7.93
172.5	18.3	45.82	1.17	120.8	142.3	9.39
		46.71	1.14	115.5	137.9	9.11
		49.95	1.17	110.8	142.3	9.39
207.0	21.96	51.15	1.16	107.3	177.9	11.75
		52.62	1.17	105.2	160.1	10.57
		54.13	1.15	100.5	164.6	10.87

TABLE V

BENDING TEST DATA FOR DACRON BEAM WITH $\rho = 17.85$

Pressure		Flexibility			Wrinkling load	
P, Pa	n, Nondim.	Force F, N	Displacement $\bar{W}$, m	Nondim. flexibility γ	F_w, N	q_w, Nondim.
34.5×10^3	3.66×10^{-3}	11.12	1.12×10^{-2}	476.5	28.9	1.91×10^{-3}
		11.12	1.13	480.8	27.8	1.84
		11.12	1.14	485.1	28.9	1.91
69.0	7.32	15.57	1.17	355.5	42.3	2.79
		16.01	1.18	348.7	46.7	3.08
		15.57	1.17	355.5	44.5	2.94
103.5	10.98	18.55	1.15	293.3	57.8	3.82
		19.44	1.17	284.8	58.9	3.89
		17.79	1.16	308.5	53.4	3.53
138.0	14.64	20.77	1.15	261.9	73.4	4.85
		21.48	1.16	255.5	75.6	4.99
		21.48	1.18	259.9	82.3	5.43
172.5	18.30	22.55	1.15	241.3	95.6	6.31
		22.24	1.14	242.5	93.4	6.17
		22.55	1.16	243.4	88.9	5.87
207.0	21.96	24.46	1.15	222.4	128.9	8.51
		25.49	1.17	217.2	120.1	7.93
		24.78	1.17	223.4	111.2	7.34

TABLE VI

BENDING TEST DATA FOR NYLON BEAM WITH $\rho = 8.4$

Pressure		Flexibility			Wrinkling load	
P, Pa	n, Nondim.	Force F, N	Displacement $\bar{W}$, m	Nondim. flexibility γ	F_w, N	q_w, Nondim.
34.5×10^3	3.11×10^{-3}	44.48	1.04×10^{-2}	130.3	84.5	4.74×10^{-3}
		45.37	1.04	127.7	82.3	4.61
		45.82	1.07	130.1	75.6	4.24
69.0	6.22	53.38	1.07	111.7	140.1	7.86
		50.26	1.00	110.9	142.3	7.98
		51.15	1.03	112.2	151.2	8.48
103.5	9.33	56.49	1.02	100.6	184.6	10.35
		62.27	1.08	96.7	193.5	10.85
		56.49	0.99	97.7	200.2	11.22
138.0	12.44	67.17	1.05	87.1	222.4	12.47
		69.39	1.07	85.9	257.9	14.46
		66.72	1.04	86.9	231.3	12.97
172.5	15.55	65.83	0.91	77.0	293.6	16.46
		65.39	0.91	77.6	240.2	13.47
		62.27	0.86	76.9	320.3	17.96
207.0	18.66	75.51	0.92	67.9	364.7	20.45
		72.06	0.90	69.6	338.1	18.96
		73.84	0.92	69.4	373.6	20.95

TABLE VII

BENDING TEST DATA FOR NYLON BEAM WITH $\rho = 14.0$

Pressure		Flexibility			Wrinkling Load	
P, Pa	n, Nondim.	Force F, N	Displacement $\overline{W}$, m	Nondim. flexibility γ	F_w, N	q_w, Nondim.
34.5×10^3	3.11×10^{-3}	19.26	1.14×10^{-2}	329.9	37.1	2.08×10^{-3}
		19.26	1.14	329.9	33.4	.87
		20.73	1.21	326.3	35.6	.99
69.0	6.22	22.51	1.17	289.7	56.9	3.19
		21.79	1.10	281.3	60.1	3.37
		22.24	1.14	285.7	57.8	3.24
103.5	9.33	22.59	1.12	276.3	90.7	5.08
		25.18	1.14	252.3	90.7	5.08
		25.49	1.14	249.2	88.9	4.98
138.0	12.44	27.80	1.14	228.5	111.2	6.23
		28.16	1.13	223.6	111.2	6.23
		28.91	1.13	217.8	122.3	6.86
172.5	15.55	31.45	1.15	203.8	140.6	7.88
		32.60	1.14	194.9	138.8	7.78
		34.83	1.15	184.0	138.8	7.78
207.0	18.66	35.58	1.13	177.0	170.4	9.55
		37.81	1.17	172.5	166.8	9.35
		37.05	1.15	172.9	166.8	9.35

TABLE VIII

BENDING TEST DATA FOR NYLON BEAM WITH ρ = 17.6

Pressure		Flexibility			Wrinkling Load	
P, Pa	n, Nondim.	Force F, N	Displacement $\bar{W}$, m	Nondim. Flexibility γ	F_w, N	q_w, Nondim.
34.5×10^3	3.11×10^{-3}	16.90	1.17×10^{-2}	385.8	26.7	1.50×10^{-3}
		17.79	1.16	363.4	26.7	1.50
		17.35	1.14	366.2	26.7	1.50
69.0	6.22	20.02	1.16	322.9	42.2	2.37
		20.02	1.16	322.9	37.8	2.12
		19.57	1.16	330.4	37.8	2.12
103.5	9.33	21.35	1.17	305.4	82.3	4.61
		21.79	1.18	301.8	60.1	3.37
		21.53	1.15	297.7	57.8	3.24
138.0	12.44	24.46	1.17	266.6	93.4	5.24
		24.91	1.16	259.5	88.9	4.98
		24.91	1.16	259.5	88.9	4.98
172.5	15.55	28.91	1.19	229.4	124.6	6.99
		29.36	1.22	231.6	122.3	6.86
		27.76	1.13	226.9	120.1	6.73
207.0	18.66	31.58	1.18	208.2	133.4	7.48
		32.21	1.20	207.6	142.3	7.98
		31.32	1.17	208.2	131.2	7.36

REFERENCES

1. Steeves, Earl C. A Linear Analysis of the Deformation of Pressure Stabilized Beams; US Army Natick Laboratories Technical Report 75–47–AMEL; 1975.

2. Foerster, A. F. Analytical and Experimental Investigation of Coated Metal Fabric Expandable Structures for Aerospace Application. AF Flight Dynamics Laboratory Report No. AST–TOR-63–542 (AD 427763); 1963.